BJR

https://doi.org/10.1259/bjr.20170318

Received: 02 May 2017 | Revised: 03 December 2017 | Accepted: 29 January 2018

Cite this article as:
Di Paola V, Cybulski A, Belluardo S, Cavicchioli F, Manfredi R, Pozzi Mucelli R. Evaluation of periprostatic neurovascular fibers before and after radical prostatectomy by means of 1.5 T MRI diffusion tensor imaging. *Br J Radiol* 2018; **91**: 20170318.

FULL PAPER

Evaluation of periprostatic neurovascular fibers before and after radical prostatectomy by means of 1.5 T MRI diffusion tensor imaging

[1]VALERIO DI PAOLA, [2]ADAM CYBULSKI, [3]SALVATORE BELLUARDO, [4]FRANCESCA CAVICCHIOLI, [1]RICCARDO MANFREDI and [2]ROBERTO POZZI MUCELLI

[1]Department of Radiology, Policlinico A. Gemelli - Università Cattolica del Sacro Cuore di Roma, Rome, Italy
[2]Department of Radiology, Policlinico G.B. Rossi - Università di Verona, Verona, Italy
[3]Department of Radiology, Ospedale Civile Maggiore di Borgo Trento – Verona, Verona, Italy
[4]Departement of Urology, Ospedale Sacro Cuore Don Calabria di Negrar, Negrar, Italy

Address correspondence to: Dr Valerio Di Paola
E-mail: *dipaola.valerio@libero.it*

Objective: To evaluate if diffusion tensor imaging (DTI) is able to detect changes of periprostatic neurovascular fibers (PNFs) before and after radical prostatectomy (RP), and if these changes are related to post-surgical urinary incontinence and erectile dysfunction.
Methods: 22 patients (mean age 62.6 years) with biopsy-proven prostate cancer underwent 1.5 T DTI before and after RP. The number, fractional anisotropy (FA) values and length of PNFs before and after RP were compared using Student's *t*-test. Each patient filled out two questionnaires before and after RP, one for the evaluation of urinary continence (ICIQ-SF) and one for the evaluation of erectile function (IIEF-5). The ratios of the number, FA values and length of PNFs before and after RP (DTI B-A RATIOs) and the ratios between the scores obtained before and after RP for both ICIQ-SF and IIEF-2 (ICIQ-SF B-A RATIOs and IIEF-2 B-A RATIOs) were calculated to perform the Kendall's τ-test between them.
Results: There was a statistically significant decrease of the number of PNFs after RP at base, midgland, and apex ($p < 0.01$) and of FA values at midgland ($p < 0.05$), with positive statistically significant correlation between the DTI B-A RATIOs of the number of PNFs and IIEF-2 B-A RATIOs ($p < 0.05$, $\rho = 0.47$).
Conclusion: DTI was able to detect that the decrease of the number of the PNFs after RP was statistically related to the post-surgical erectile dysfunction ($p < 0.05$).
Advances in knowledge: This work demonstrates that: (1) 1.5 T MRI DTI is able to detect the decrease of the number and of the FA of PNFs after prostatectomy; (2) the decrease of the number of PNFs after prostatectomy is related with the post-surgical erectile dysfunction; (3) 1.5 T MRI DTI has demonstrated to be a reproducible technique in detecting the changes of the PNFs induced by RP, with high interobserver agreement.

INTRODUCTION

Prostate cancer is the more common malignant neoplasm in males, accounting for 25% of all tumors and the second cause of death due to cancer.[1]

Currently, radical prostatectomy (RP) represents the treatment of choice of locally advanced prostatic cancer, but is burdened with complications such as urinary incontinence and erectile dysfunction. RP provides excellent long-term disease control for patients with clinically localized prostate carcinoma,[2] aiming to a complete excision of the tumor.[3] Unfortunately, even if the recent introduction of "nerve-sparing" techniques has reduced the incidence of both urinary incontinence and erectile dysfunction in comparison with "non nerve-sparing" approaches,[4–7] their incidence is still not negligible: it varies from 42 to 89% after unilateral nerve-sparing and from 18 to 32% after bilateral nerve-sparing surgery.[8]

The need to avoid these complications has become more and more challenging because of the younger age of the diagnosis of prostate cancer in the last three decades. In fact, after the introduction of PSA screening in 1986, the incidence doubled from 350 to 667 per 100,000 for males aged 60–69 years and tripled from 59 to 216 per 100,000 for males aged 50–59 years.[9]

In this scenario, the visualization of the PNFs represents an emerging issue in the post-surgical evaluation of the effects induced by surgery on the PNFs.[2] It has been

Table 1. MRI protocol

Pulse sequence	Plane	Repetition & echo time (ms)	Section thickness (mm)	FOV (mm)	Flip angle	Duration	Acquisition matrix	Sense factor
T2 TSE	Axial	4100/100	4	380 × 340	90°	1′30″	336 × 327	2
T2 TSE (HR)	Sagittal	2650/90	3.5	200 × 200	90°	1′40″	256 × 195	2
T2 TSE (HR)	Coronal	2500/100	3.5	160 × 160	90°	3′25″	288 × 228	2
T2 TSE (HR)	Axial	3730/90	3.5	160 × 160	90°	4′10″	288 × 240	2
DWI	Axial	4000/90	3.5	300 × 300	90°	7′47″	120 × 120	2
DTI	Axial	1449/88	3	220 × 220	90°	3′14″	76 × 72	2
T1 DIXON Ddynamic phase	Axial	4/2	3.5	200 × 220	10°	3′17″	256 × 256	\
b-SSFP	Axial	5000/80	6	400 × 350	90°	51′	272 × 241	1.2

b-SSFP, balanced steady state free precession; DTI, diffusion tensor imaging; DWI, diffusion weighted imaging; HR, high resolution; TSE, turbo spin echo.

demonstrated that the recovery of erectile function after RP is directly related to the number of preserved periprostatic neurovascular fibers (PNFs) during RP.[10,11] Even if MRI is the recommended imaging modality for diagnosis, staging and follow up of prostate cancer[12–16] with high accuracy in the evaluation of extracapsular invasion of prostate cancer,[17,18] the visualization of the PNFs remains still difficult. In a study of 93 patients who underwent bilateral nerve-sparing RP, pre-operative conventional T_2 weighted MRI visualized the PNFs in only 37.6% of patients.[19]

Nowadays, diffusion tensor imaging (DTI) is an emerging and non-invasive MRI modality in the field of neuroimaging that provides a successful depiction of central and peripheral nervous fibers.[20–30] In particular, this technique has been used for the neurosurgical planning in the removal of brain tumors[22], as well as for the depiction of neural pathway in the mapping of the brain, spinal cord and brachial plexus.[30] More recently, DTI has been introduced as useful imaging modality in the mapping of the PNFs.[2,31,32] DTI is based on the sensitivity to "anisotropic diffusion" of the water protons in the biological tissues with a strictly orientated texture, such as nervous central and peripheral fibers, including the PNFs.[20] In this kind of tissues, the water protons diffusion is not casual or "Brownian", but oriented along a determined axis or "anisotropic".[33] Throughout the measurement of fractional anisotropy (FA) for each single voxel in, at least six non-collinear and non-coplanar directions, DTI is able to quantify the phenomenon of anistropic diffusion. Then, by the integration of FA values of all voxels, it becomes possible to depict the direction of nervous fibers in all three dimensions of space, giving both quantitative and qualitative anatomic information.

Therefore, the aim of the present study was to evaluate if DTI is able to detect changes of the PNFs before and after RP, and if these changes are related to post-surgical complications, such as urinary incontinence and erectile dysfunction.

METHODS AND MATERIALS

Patient population

This prospective study was approved by our institutional review board, and included male patients with biopsy-proven prostate cancer candidate to RP, who gave their written informed consent to MRI examination. Conversely, patients with absolute contraindications to perform an MRI examination or patients who did not give their consent were excluded from the study; moreover, post-surgical or post-biopsy bleeding (hyperintensity on T_1 weighted images) and death were also considered as exclusion criteria.

Thus, our study population consisted of 22 patients (mean age 62.6 years), who underwent 1.5 T MRI including DTI before and after RP between October 2014 and May 2016. The mean interval between pre-RP DTI and RP was 30 days (range: 1–129 days), while the mean interval between RP and post-RP DTI was 132 days (range: 27–434 days). Furthermore, the mean interval between pre-RP DTI and biopsy was 44 days (range: 22–68 days).

Figure 1. (a) Placing of ROIs on the fused T_2-DTI images in the periprostatic fat tissue at base (a), mid gland (b) and apex (c) before radical prostatectomy. (b) Placing of ROIs on the fused T_2-DTI images in the periprostatic fat tissue at base (d), mid gland (e) and apex (f) after radical prostatectomy. ROIs, regions of interest.

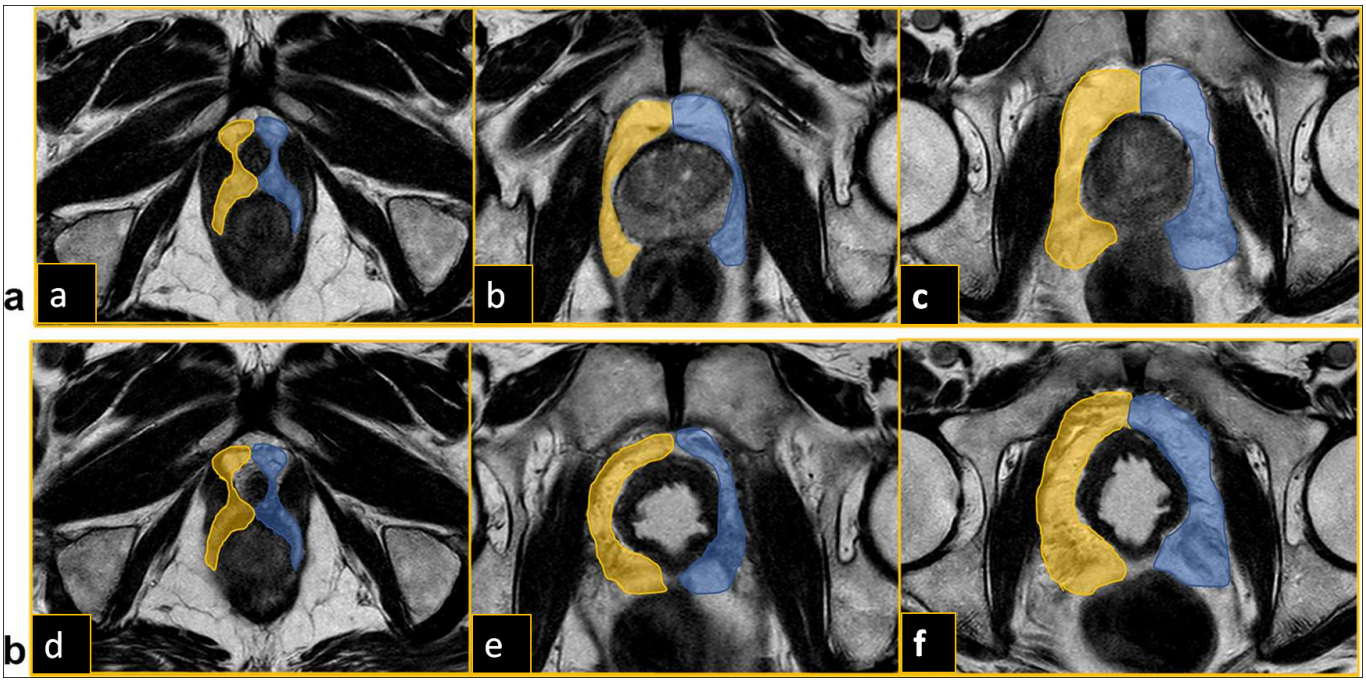

MRI

Before the MRI examination, we asked the patients to fast from solid food since 4–6 h and administrated intramuscularly 20 mg of scopolamine butyl bromide (Buscopan; Boehringer Ingelheim, Yamagata, Japan) to suppress intestinal peristalsis. Moreover, we asked the patients to have half-filled bladder to limit involuntary movements.

All patients were scanned with a 1.5 T MR unit (Ingenia; Philips Medical Systems, Eindhoven, Netherlands) using a multichannel phased array (32-channel coil) for signal reception, without using endorectal coil.

MRI protocol (Table 1) consisted of T_2 weighted turbo spin echo (TSE) images (slice thickness 4 mm) on axial plane, high resolution T_2 weighted TSE images on axial, sagittal and coronal plane (slice thickness 3.5 mm), and diffusion-weighted images on axial plane (slice thickness 3 mm, b-value = 0, 800 s mm^{-2}). After standard anatomical TSE and diffusion-weightedimaging sequences, the DTI was acquired in 32 directions (repetition time/echo time 1449/88 ms, thickness 3 mm, b-value = 0, 800 s mm^{-2}), with a scan duration for DTI sequence of 3 min and 14 s. At last, the dynamic imaging was performed during gadolinium chelate injection (0.1 mmol per kg of body weight gadolinium chelates, MultiHance®, Bracco Imaging, Milan, Italy; Gadovist®, Schering, Berlin, Germany) with a power injector (Medrad® Spectris Solaris®; Medrad, Pittsburgh, PA) at a rate of 2 ml s^{-1}. The dynamic imaging was acquired only for pre-RP MRI examinations and consisted of the repetition of 14 T_1 DIXON acquisitions after contrast injection, while for post-RP MRI examinations only one T_1 DIXON acquisition was performed without medium contrast administration.

Surgery

Robotic-assisted radical prostatectomy with the retrograde approach was performed in 22/22 patients (100%), with nerve-sparing technique in 12/22 (54%) patients and non-nerve sparing technique in 10/22 (46%) patients. The nerve-sparing technique was performed through the intrafascial approach (2/12), if the plane of dissection was performed between the prostatic capsule and the prostatic fascia or through the interfascial approach (10/12), if the plane of dissection was performed between the prostatic fascia and the lateral pelvic fascia.[34–36] In the extrafascial non nerve-sparing technique, the plane of dissection was performed laterally to the lateral pelvic fascia.

Moreover, the extended pelvic lymphadenectomy was performed in 2/22 (9%) patients, while bladder–urethral anastomosis was performed using a continuous suture.[37]

Image analysis

MR images were analyzed by two radiologists (VDP, AJC with 7 and 5 years experience in prostate imaging), who independently performed their own post-processing tractographic reconstruction of PNFs on each single MRI examination. The reconstruction was performed by using the Fiber Tracking Software provided by Philips (v. 4.1), which consisted of a deterministic tracking algorithm based on the criterion of linear propagation using the following parameters: angle threshold of 45°, FA threshold of 0.15 and minimum length threshold of 5 mm, analogously to other published studies.[30,31]

In the DTI post-processing phase, the DTI images were synchronized with the axial T_2 weighted images to correct

Table 2. Mean values and standard deviation of the number, of the FA values and of the length (mm) of the fiber tracts before and after radical prostatectomy at base, midgland, and apex levels for right and left side, with relative DTI B-A RATIOs and *p*-value

Number						
	Base		Midgland		Apex	
	right	left	right	left	right	left
Before-RP	152 ± 40	153 ± 42	115 ± 34	120 ± 35	41 ± 17	42 ± 19
After-RP	111 ± 41	113 ± 51	86 ± 30	84 ± 40	25 ± 11	26 ± 13
DTI B-A RATIOs	1.5	1.6	1.5	1.9	1.9	1.7
***p*-value**	**<0.01**	**<0.01**	**<0.01**	**<0.01**	**<0.01**	**<0.01**
Fractional anisotropy (FA)						
	Base		Midgland		Apex	
	right	left	right	left	right	left
Before-RP	0.431 ± 0.060	0.416 ± 0.057	0.450 ± 0.053	0.444 ± 0.063	0.319 ± 0.043	0.324 ± 0.045
After-RP	0.430 ± 0.063	0.417 ± 0.064	0.414 ± 0.052	0.406 ± 0.055	0.315 ± 0.046	0.304 ± 0.041
DTI B-A RATIOs	1.0	1.0	1.1	1.1	1.0	1.1
***p*-value**	0.96	0.96	**<0.05**	**<0.05**	0.13	0.74
Length (mm)						
	Base		Midgland		Apex	
	right	left	right	left	right	left
Before-RP	12.3 ± 0.3	12.4 ± 0.03	12.1 ± 2.5	12.2 ± 1.6	13.8 ± 0.8	14.7 ± 0.1
After-RP	12.2 ± 1.6	12.1 ± 1.5	12.1 ± 1.5	11.7 ± 1.2	13.2 ± 2.8	13.4 ± 2.5
DTI B-A RATIOs	1.0	1.0	1.0	1.0	1.1	1.1
***p*-value**	0.82	0.61	0.96	0.28	0.51	0.17

DTI B-A RATIOs, ratio between numbers, FA values and length of the fiber tracts before and after radical prostatectomy; RP, radical prostatectomy.

Figure 2. Number of fiber tracts at base (a), midgland (b) and apex (c) before radical prostatectomy: they were significantly lower ($p < 0.01$) after radical prostatectomy at base (d), at mid gland (e) and at apex (f).

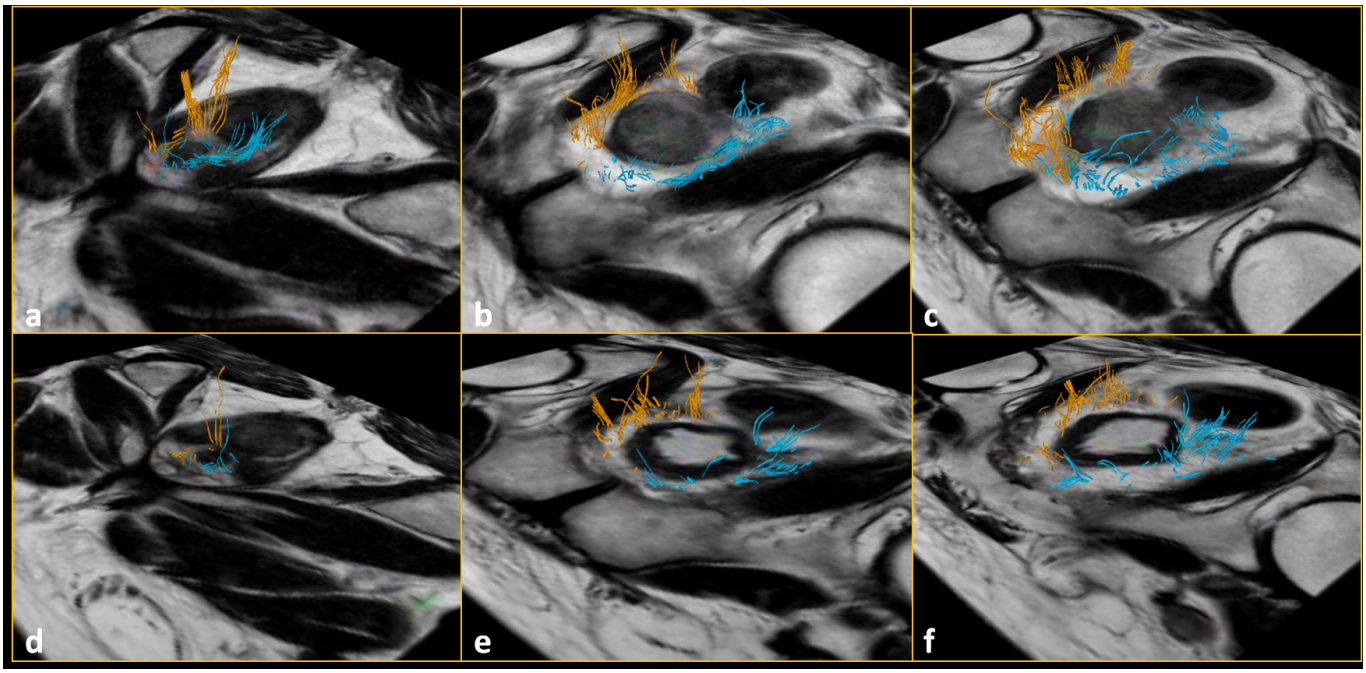

Figure 3. Decrease of the number of fiber tracts after radical prostatectomy (RP) at base, mid gland, and apex on right (R) and left (L) side. FA values after RP at mid gland on right and left side. RP, radical prostatectomy; R, right; L, left

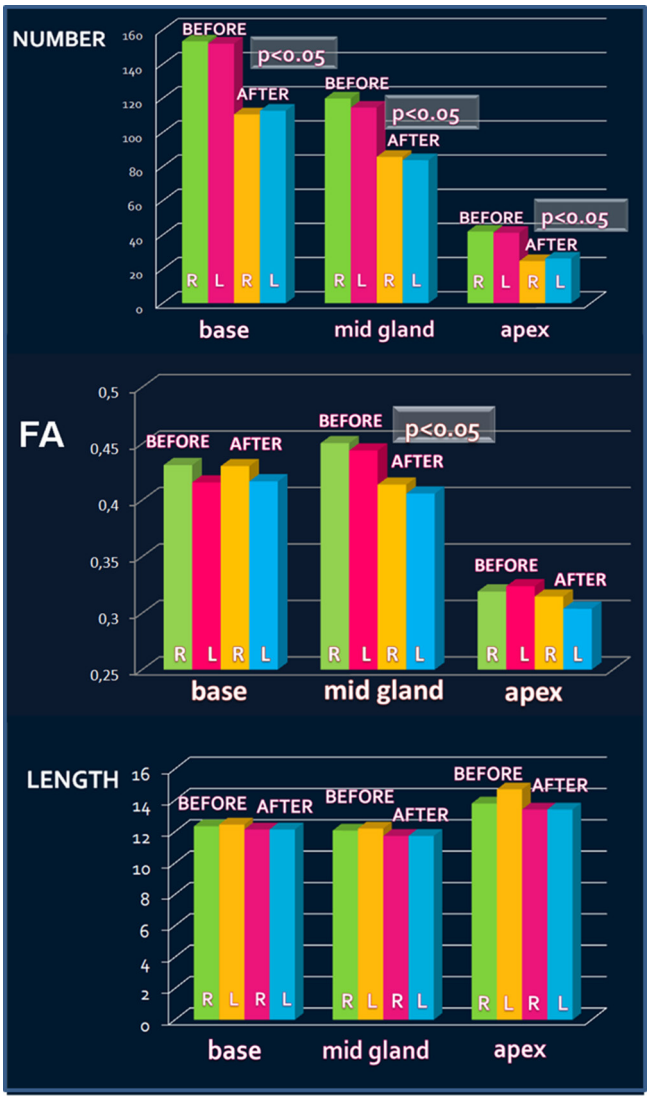

eventual movement artifacts of the patients; subsequently, the axial T_2 weighted images were fused with the synchronized DTI images, obtaining a T_2 weighted-DTI hybrid images. On these fused T_2/DTI images, the regions of interest were drawn by each observer in the periprostatic fat tissue tangentially to prostatic capsule and wall bladder, to avoid that fibromuscular fibers were included in the reconstruction. Both observers placed independently six regions of interest in the periprostatic fat tissue at base, midgland and apex, both on the right and the left side before (Figure 1a) and after RP (Figure 1b).

After software elaboration, the number, the FA and ADC values and the length in millimeters were calculated for each reconstructed fiber tract at base, midgland, apex both on the right and the left side before and after RP.

Quantitative analysis

Then, the numbers, the FA values and the length of the fiber tracts before and after RP were compared using Student's *t*-test at the base, midgland, and apex levels for both right and left side to evaluate if there were statistically significant differences between these values before and after RP. The ratio between numbers, the FA values and the length of the fiber tracts before and after RP was also calculated for all these localizations (DTI B-A RATIOs).

Correlation with urinary incontinence and erectile dysfunction

Each patient were asked to fill out two questionnaires before and after RP, one for the evaluation of urinary continence (ICIQ-SF),[38] and one for the evaluation of erectile function (IIEF-5).[39] The ratios between the scores obtained before and the score obtained after RP for both ICIQ-SF and IIEF-2 was also calculated (ICIQ-SF B-A RATIOs and IIEF-2 B-A RATIOs).

Subsequently, the Kendall's τ-test was performed between the DTI B-A RATIOs of the total number, of the FA values and of the length of the fiber tracts, and both the ICIQ-SF B-A RATIOs and the IIEF-2 B-A RATIOs to evaluate if there was a statistically significant correlation between the changes of the fiber tracts after RP and both urinary incontinence and erectile dysfunction.

Interobserver agreement

The interobserver agreement for the number, for the FA values and for the length of the fiber tracts before and after RP was assessed by means of intraclass correlation coefficient (ICC): a value of 0.20 indicated poor agreement; a value of 0.21–0.40, fair agreement; a value of 0.41–0.60, moderate agreement; a value of 0.61–0.80, good agreement; and a value of 0.81–1.00, excellent agreement.

Repeatability

Bias and limits of agreement of the repeated DTI measurements were assessed by both observers via Bland–Altman analysis. These analyses were applied to the number, FA values and fiber tracts lengths before and after RP.

RESULTS

The mean values of the numbers, the FA values and of the length of fiber tracts before and after RP at base, midgland, and apex levels for right and left side, with relative DTI B-A RATIOs and *p*-values are reported in Table 2.

The number of fiber tracts decreased after RP at base, midgland, and apex for both right and left side (Figure 2); the decrease was statistically significant for all these sites ($p < 0.01$) (Figure 3).

The FA values at midgland showed a decrease after RP from 0.450 to 0.414 on the right side and from 0.444 to 0.406 on the left side, with statistically significant difference ($p < 0.05$) (Figure 3). No statistically significant differences were found for the FA values at base and apex. The length of the fibers did not show any statistically significant differences (Figure 3).

Table 3. ICIQ-SF scores sand IIEF-2 scores before and after radical prostatectomy and their relative B-A RATIOs

ICIQ-SF pre	IIEF-2 pre	ICIQ-SF post	IIEF-2 post	ICIQ-SF B-A RATIOs	IIEF-2 B-A RATIOs
1	25	7	1	7	25
1	10	9	2	9	5
1	21	9	1	9	21
1	16	9	5	9	3.2
1	25	1	17	1	1.5
1	23	11	1	11	23
1	20	22	1	22	20
1	25	5	12	5	2.1
1	25	7	17	7	1.5
1	25	9	1	9	25
1	21	8	1	8	21
1	25	16	1	16	25
1	25	8	19	8	1.3
1	25	11	1	11	25
1	25	13	9	13	2.8
1	24	20	1	20	24
1	24	11	7	11	3.4
1	20	5	5	5	4
1	25	1	6	1	4.2
1	25	7	8	7	3.1
1	25	4	22	4	1.1
1	10	4	1	4	10

B-A RATIOs, ratio before/after radical prostatectomy.

Correlation with urinary incontinence and erectile dysfunction

The scores of the two questionnaires (ICIQ-SF and IIEF-2) before and after RP and their relative B-A RATIOs are reported in Table 3.

Figure 4. Correlation between the DTI B-A RATIOs of the number of fiber tracts and IIEF-2 B-A RATIOs ($p < 0.05$, $\tau = 0.35$). B-A RATIOs = ratio before/after radical prostatectomy. DTI, diffusion tensor imaging.

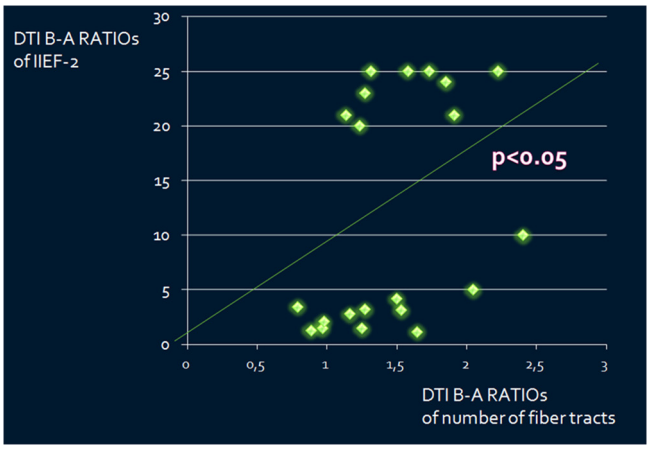

There was a positive statistically significant correlation between the DTI B-A RATIOs of the number of fiber tracts and IIEF-2 B-A RATIOs ($p < 0.05$, $\tau = 0.35$) (Figure 4).

No statistically significant correlations were found between the DTI B-A RATIOs of the FA values and of the length of the fiber tracts and the IIEF-2 B-A RATIOs, neither between the DTI B-A RATIOs of the number, of the FA values and of the length of the fiber tracts and ICIQ-SF B-A RATIOs.

Interobserver agreement

The interobserver agreement values before and after RP were: 0.82 and 0.61 for the number, 0.92 and 0.73 for FA values, 0.96 and 0.75 for the length of the fibers.

Repeatability

The Bland–Altman analysis for the number, for the FA values and for the length of the fiber tracts before and after RP showed that all data points were included within the limits of agreement (Figure 5a,b). The bias detected on the basis of the measured limits of agreement appears to be not clinically important (Table 4).

Figure 5. (a) Bland–Altman plots (with 95% confidence interval) of the two repeated DTI measurements of Observer 1 for the number, the FA values and the length of the fiber tracts before and after radical prostatectomy. *x*-axis = mean of first and second measurement of Observer 1. *y*-axis = differences between first and second measurement of Observer 1. (b) Bland–Altman plots (with 95% confidence interval) of the two repeated DTI measurements of Observer 2 for the number, the FA values and the length of the fiber tracts before and after radical prostatectomy. *x*-axis = mean of first measurement and second measurement of Observer 2. *y*-axis = differences between first and second measurement of Observer 2. DTI, diffusion tensor imaging; FA, fractional anisotropy.

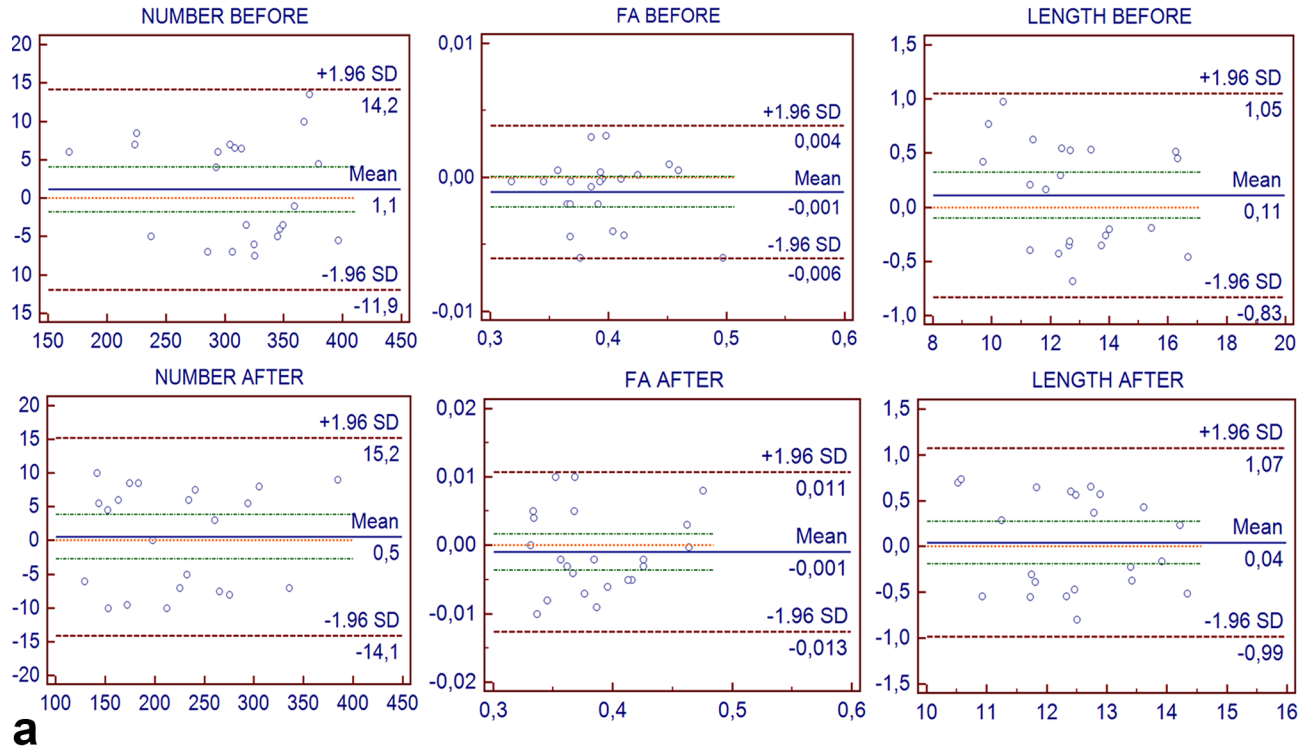

Table 4. Mean difference, standard deviation, upper and lower limits of agreement of the repeated DTI measurements assessed by both observers via Bland–Altman analysis for number, FA and length of fiber tracts before and after prostatectomy

	Number before	Number after	FA before	FA after	Length before	Length after
Mean difference	1.1	0.5	−0.001	−0.001	0.1	0.0
Standard deviation	6.6	7.5	0.002	0.006	0.5	0.5
Lower limits	−11.9	−14.1	−0.006	−0.013	−0.8	−1.0
Upper limits	14.2	15.2	0.004	0.011	1.0	1.1
Mean difference	2.2	0.9	0.000	−0.004	0.1	0.0
Standard deviation	6.9	6.4	0.002	0.007	0.5	0.5
Lower limits	−11.3	−11.7	−0.003	−0.017	−0.9	−0.9
Upper limits	15.7	13.5	0.004	0.010	1.0	0.8

DTI, diffusion tensor imaging; FA, fractional anisotropy.

DISCUSSION

The aim of the present study was to evaluate, if DTI is able to detect the changes of the PNFs before and after prostatectomy, and if these changes are related to post-surgical complications, such as urinary incontinence and erectile dysfunction.

The total number of the fiber tracts was similar to other published studies performed by means of a 3 T scanner and endorectal coil,[2,31] with 623 fiber tracts of our series *vs* 730 of Kitajima et al series and 875 of Finley et al series,[2,31] decreasing from the base (152 for right side and 151 for left side) to midgland (115 and 120) and apex (41 and 42), with slightly asymmetric distribution between the two sides in each patient.

In agreement with Kitajima et al[2] in our study, the number of fiber tracts was significantly decreased after RP at base, midgland, and apex for both right and left side ($p < 0.01$), and this decrease showed a statistically significant correlation with the decrease of erectile function after RP ($p < 0.05$). This result indicates that the decrease of the number of fiber tracts after RP may have a role in the post-surgical erectile dysfunction, as suggested by Kitajima et al series, in which the reduction of the number of the PNFs was higher in patients, who underwent non-nerve sparing prostatectomy in respect of patients who underwent nerve-sparing prostatectomy.[2]

Another interesting result of our study, which has not ever studied before was represented by the statistically significant decrease of the FA values at midgland after RP from 0.450 to 0.414 on right side and from 0.444 to 0.406 on left side ($p < 0.05$). This data suggest that the fibers after RP are less oriented and more disarranged, analogously to other published studies which have demonstrated a decrease of the FA values in several neurological diseases.[40–42] In our study, the lower FA values were associated with higher ADC values in each analyzed area (base, midgland and apex), probably because the decrease of the number of fiber tracts and their increased disarrangement induced a higher water molecules diffusion. Another possible factor which may concur to reduce the FA values of the PNFs is the traction performed on them during the surgical dissection of the prostate gland, a condition which is known as potential cause of the so called "neuroapraxia".[43]

No correlations were found between the number, the FA values and the length of the fibers and urinary incontinence, probably because other factors in addition to neurovascular damage may concur to post-RP incontinence, such as the damage of the urethral sphincter during the apical dissection and the urethral length post-RP.[44]

A further important result of our study was represented by the high interobserver agreement values, demonstrating that DTI of the PNFs is reliable technique. Moreover, neither the bias nor limits of agreement between DTI output metrics across repeated assessments were not clinically important for either observer, suggesting the potential repeatability of the technique. However, repeated DTI acquisitions under the same conditions were not performed.

The main limitations of the present study were the lack of a gold-standard anatomical correlation, the potential miscount of nerve fibers because of the presence of linear non-nerve structures (fibromuscular tissue, arteries and veins) and the relatively small number of patient included in the study.

In conclusion, 1.5 T MRI DTI has demonstrated to be a useful and reproducible technique in detecting a statically significant decrease of the number ($p < 0.01$) and of the FA values ($p < 0.05$) of the PNFs after RP. The decrease of the number of PNFs after RP was statistically related to the decrease of post-surgical erectile function ($p < 0.05$), suggesting that this could be an important factor related to the post-surgical erectile dysfunction.

REFERENCES

1. Claus FG, Hricak H, Hattery RR. Pretreatment evaluation of prostate cancer: role of MR imaging and 1H MR spectroscopy. *Radiographics* 2004; **24**(Suppl 1): S167–S180. doi: https://doi.org/10.1148/24si045516
2. Kitajima K, Takahashi S, Ueno Y, Miyake H, Fujisawa M, Sugimura K. Visualization of periprostatic nerve fibers before and after radical prostatectomy using diffusion tensor magnetic resonance imaging with tractography. *Clin Imaging* 2014; **38**: 302–6. doi: https://doi.org/10.1016/j.clinimag.2014.01.009
3. Menon M, Shrivastava A, Kaul S, Badani KK, Fumo M, Bhandari M, et al. Vattikuti Institute prostatectomy: contemporary technique and analysis of results. *Eur Urol* 2007; **51**: 648–58. doi: https://doi.org/10.1016/j.eururo.2006.10.055
4. Takenaka A, Leung RA, Fujisawa M, Tewari AK. Anatomy of autonomic nerve component in the male pelvis: the new concept from a perspective for robotic nerve sparing radical prostatectomy. *World J Urol* 2006; **24**: 136–43. doi: https://doi.org/10.1007/s00345-006-0102-2
5. Chabert CC, Merrilees DA, Neill MG, Eden CG. Curtain dissection of the lateral prostatic fascia and potency after laparoscopic radical prostatectomy: a veil of mystery. *BJU Int* 2008; **101**: 1285–8. doi: https://doi.org/10.1111/j.1464-410X.2008.07595.x
6. Vora AA, Marchalik D, Kowalczyk KJ, Nissim H, Bandi G, McGeagh KG, et al. Robotic-assisted prostatectomy and open radical retropubic prostatectomy for locally-advanced prostate cancer: multi-institution comparison of oncologic outcomes. *Prostate Int* 2013; **1**: 31–6. doi: https://doi.org/10.12954/PI.12001
7. Labanaris AP, Witt JH, Zugor V. Robotic-assisted radical prostatectomy in men ≥75 years of age. Surgical, oncological and functional outcomes. *Anticancer Res* 2012; **32**: 2085–9.
8. Kiyoshima K, Yokomizo A, Yoshida T, Tomita K, Yonemasu H, Nakamura M, et al. Anatomical features of periprostatic tissue and its surroundings: a histological analysis of 79 radical retropubic prostatectomy specimens. *Jpn J Clin Oncol* 2004; **34**: 463–8. doi: https://doi.org/10.1093/jjco/hyh078
9. Welch HG, Albertsen PC. Prostate cancer diagnosis and treatment after the introduction of prostate-specific antigen screening: 1986-2005. *J Natl Cancer Inst* 2009; **101**: 1325–9. doi: https://doi.org/10.1093/jnci/djp278
10. Ko WJ, Truesdale MD, Hruby GW, Landman J, Badani KK. Impacting factors for recovery of erectile function within 1 year following robotic-assisted laparoscopic radical prostatectomy. *J Sex Med* 2011; **8**: 1805–12. doi: https://doi.org/10.1111/j.1743-6109.2011.02237.x
11. Rabbani F, Stapleton AM, Kattan MW, Wheeler TM, Scardino PT. Factors predicting recovery of erections after radical prostatectomy. *J Urol* 2000; **164**: 1929–34. doi: https://doi.org/10.1016/S0022-5347(05)66921-2
12. Guneyli S, Erdem CZ, Erdem LO. Magnetic resonance imaging of prostate cancer. *Clin Imaging* 2016; **40**: 601–9. doi: https://doi.org/10.1016/j.clinimag.2016.02.011
13. Yakar D, Debats OA, Bomers JG, Schouten MG, Vos PC, van Lin E, et al. Predictive value of MRI in the localization, staging, volume estimation, assessment of aggressiveness, and guidance of radiotherapy and biopsies in prostate cancer. *J Magn Reson Imaging* 2012; **35**: 20–31. doi: https://doi.org/10.1002/jmri.22790
14. Bomers JG, Barentsz JO. Standardization of multiparametric prostate MR imaging using PI-RADS. *Biomed Res Int* 2014; **2014**: 431680–. doi: https://doi.org/10.1155/2014/431680
15. Sciarra A, Barentsz J, Bjartell A, Eastham J, Hricak H, Panebianco V, et al. Advances in magnetic resonance imaging: how they are changing the management of prostate cancer. *Eur Urol* 2011; **59**: 962–77. doi: https://doi.org/10.1016/j.eururo.2011.02.034
16. Turkbey B, Choyke PL. Multiparametric MRI and prostate cancer diagnosis and risk stratification. *Curr Opin Urol* 2012; **22**: 310–5. doi: https://doi.org/10.1097/MOU.0b013e32835481c2
17. Hricak H, Wang L, Wei DC, Coakley FV, Akin O, Reuter VE, et al. The role of preoperative endorectal magnetic resonance imaging in the decision regarding whether to preserve or resect neurovascular bundles during radical retropubic prostatectomy. *Cancer* 2004; **100**: 2655–63. doi: https://doi.org/10.1002/cncr.20319
18. McClure TD, Margolis DJ, Reiter RE, Sayre JW, Thomas MA, Nagarajan R, et al. Use of MR imaging to determine preservation of the neurovascular bundles at robotic-assisted laparoscopic prostatectomy. *Radiology* 2012; **262**: 874–83. doi: https://doi.org/10.1148/radiol.11103504
19. Lee SE, Hong SK, Han JH, Han BK, Yu JH, Jeong SJ, et al. Significance of neurovascular bundle formation observed on preoperative magnetic resonance imaging regarding postoperative erectile function after nerve-sparing radical retropubic prostatectomy. *Urology* 2007; **69**: 510–4. doi: https://doi.org/10.1016/j.urology.2006.11.008
20. Le Bihan D, Breton E, Lallemand D, Grenier P, Cabanis E, Laval-Jeantet M. MR imaging of intravoxel incoherent motions: application to diffusion and perfusion in neurologic disorders. *Radiology* 1986; **161**: 401–7. doi: https://doi.org/10.1148/radiology.161.2.3763909
21. Ahn S, Lee SK. Diffusion tensor imaging: exploring the motor networks and clinical applications. *Korean J Radiol* 2011; **12**: 651–61. doi: https://doi.org/10.3348/kjr.2011.12.6.651
22. Yu CS, Li KC, Xuan Y, Ji XM, Qin W. Diffusion tensor tractography in patients with cerebral tumors: a helpful technique for neurosurgical planning and postoperative assessment. *Eur J Radiol* 2005; **56**: 197–204. doi: https://doi.org/10.1016/j.ejrad.2005.04.010
23. Jones DK. The effect of gradient sampling schemes on measures derived from diffusion tensor MRI: a Monte Carlo study. *Magn Reson Med* 2004; **51**: 807–15. doi: https://doi.org/10.1002/mrm.20033
24. Yamada K, Kizu O, Mori S, Ito H, Nakamura H, Yuen S, et al. Brain fiber tracking with clinically feasible diffusion-tensor MR imaging: initial experience. *Radiology* 2003; **227**: 295–301. doi: https://doi.org/10.1148/radiol.2271020313
25. Okada T, Miki Y, Fushimi Y, Hanakawa T, Kanagaki M, Yamamoto A, et al. Diffusion-tensor fiber tractography: intraindividual comparison of 3.0-T and 1.5-T MR imaging. *Radiology* 2006; **238**: 668–78. doi: https://doi.org/10.1148/radiol.2382042192
26. Kulikova S, Hertz-Pannier L, Dehaene-Lambertz G, Buzmakov A, Poupon C, Dubois J. Multi-parametric evaluation of the white matter maturation. *Brain Struct Funct* 2015; **220**: 3657–72. doi: https://doi.org/10.1007/s00429-014-0881-y
27. Löbel U, Sedlacik J, Güllmar D, Kaiser WA, Reichenbach JR, Mentzel HJ. Diffusion tensor imaging: the normal evolution of ADC, RA, FA, and eigenvalues studied in multiple anatomical regions of the brain. *Neuroradiology* 2009; **51**: 253–63. doi: https://doi.org/10.1007/s00234-008-0488-1
28. Fabri M, Pierpaoli C, Barbaresi P, Polonara G. Functional topography of the

corpus callosum investigated by DTI and fMRI. *World J Radiol* 2014; **6**: 895–906. doi: https://doi.org/10.4329/wjr.v6.i12.895

29. Lin CC, Tsai MY, Lo YC, Liu YJ, Tsai PP, Wu CY, et al. Reproducibility of corticospinal diffusion tensor tractography in normal subjects and hemiparetic stroke patients. *Eur J Radiol* 2013; **82**: e610–e616. doi: https://doi.org/10.1016/j.ejrad.2013.06.016
30. Vargas MI, Viallon M, Nguyen D, Delavelle J, Becker M, imaging Dtensor. Diffusion tensor imaging (DTI) and tractography of the brachial plexus: feasibility and initial experience in neoplastic conditions. *Neuroradiology* 2010; **52**: 237–45. doi: https://doi.org/10.1007/s00234-009-0643-3
31. Finley DS, Ellingson BM, Natarajan S, Zaw TM, Raman SS, Schulam P, et al. Diffusion tensor magnetic resonance tractography of the prostate: feasibility for mapping periprostatic fibers. *Urology* 2012; **80**: 219–23. doi: https://doi.org/10.1016/j.urology.2012.03.027
32. Panebianco V, Barchetti F, Sciarra A, Marcantonio A, Zini C, Salciccia S, et al. In vivo 3D neuroanatomical evaluation of periprostatic nerve plexus with 3T-MR Diffusion Tensor Imaging. *Eur J Radiol* 2013; **82**: 1677–82. doi: https://doi.org/10.1016/j.ejrad.2013.05.013
33. Farrell JA, Landman BA, Jones CK, Smith SA, Prince JL, van Zijl PC, et al. Effects of signal-to-noise ratio on the accuracy and reproducibility of diffusion tensor imaging-derived fractional anisotropy, mean diffusivity, and principal eigenvector measurements at 1.5 T. *J Magn Reson Imaging* 2007; **26**: 756–67. doi: https://doi.org/10.1002/jmri.21053
34. Tewari AK, Srivastava A, Huang MW, Robinson BD, Shevchuk MM, Durand M, et al. Anatomical grades of nerve sparing: a risk-stratified approach to neural-hammock sparing during robot-assisted radical prostatectomy (RARP). *BJU Int* 2011; **108**: 6 Pt 2: 984–92. doi: https://doi.org/10.1111/j.1464-410X.2011.10565.x
35. Schatloff O, Chauhan S, Sivaraman A, Kameh D, Palmer KJ, Patel VR. Anatomic grading of nerve sparing during robot-assisted radical prostatectomy. *Eur Urol* 2012; **61**: 796–802. doi: https://doi.org/10.1016/j.eururo.2011.12.048
36. Tavukçu HH, Aytac O, Atug F. Nerve-sparing techniques and results in robot-assisted radical prostatectomy. *Investig Clin Urol* 2016; **57**(Suppl 2): S172–S84. doi: https://doi.org/10.4111/icu.2016.57.S2.S172
37. Van Velthoven RF, Ahlering TE, Peltier A, Skarecky DW, Clayman RV. Technique for laparoscopic running urethrovesical anastomosis:the single knot method. *Urology* 2003; **61**: 699–702. doi: https://doi.org/10.1016/S0090-4295(02)02543-8
38. Seckiner I, Yesilli C, Mungan NA, Aykanat A, Akduman B. Correlations between the ICIQ-SF score and urodynamic findings. *Neurourol Urodyn* 2007; **26**: 492–4. doi: https://doi.org/10.1002/nau.20389
39. Rosen RC, Cappelleri JC, Smith MD, Lipsky J, Peña BM. Development and evaluation of an abridged, 5-item version of the international index of erectile function (IIEF-5) as a diagnostic tool for erectile dysfunction. *Int J Impot Res* 1999; **11**: 319–26. doi: https://doi.org/10.1038/sj.ijir.3900472
40. Filippi M, Cercignani M, Inglese M, Horsfield MA, Comi G. Diffusion tensor magnetic resonance imaging in multiple sclerosis. *Neurology* 2001; **56**: 304–11. doi: https://doi.org/10.1212/WNL.56.3.304
41. Beppu T, Inoue T, Shibata Y, Kurose A, Arai H, Ogasawara K, et al. Measurement of fractional anisotropy using diffusion tensor MRI in supratentorial astrocytic tumors. *J Neurooncol* 2003; **63**: 109–16. doi: https://doi.org/10.1023/A:1023977520909
42. Ward P, Counsell S, Allsop J, Cowan F, Shen Y, Edwards D, et al. Reduced fractional anisotropy on diffusion tensor magnetic resonance imaging after hypoxic-ischemic encephalopathy. *Pediatrics* 2006; **117**: e619–e630. doi: https://doi.org/10.1542/peds.2005-0545
43. Lei Y, Alemozaffar M, Williams SB, Hevelone N, Lipsitz SR, Plaster BA, et al. Athermal division and selective suture ligation of the dorsal vein complex during robot-assisted laparoscopic radical prostatectomy: description of technique and outcomes. *Eur Urol* 2011; **59**: 235–43. doi: https://doi.org/10.1016/j.eururo.2010.08.043
44. Hoyland K, Vasdev N, Abrof A, Boustead G. Post-radical prostatectomy incontinence: etiology and prevention. *Rev Urol* 2014; **16**: 181–8.